Available online at www.sciencedirect.com

SCIENCE DIRECT®

International Journal of Mass Spectrometry 242 (2005) 97–115

www.elsevier.com/locate/ijms

The development of multiple collector mass spectrometry for isotope ratio measurements

Michael E. Wieser[a,*], Johannes B. Schwieters[b]

[a] Department of Physics and Astronomy, University of Calgary, 2500 University Drive N.W., Calgary, AB, Canada T2N 1N4
[b] Thermo Electron (Bremen) GmbH, Hanna-Kunath-Str. 11, 28199 Bremen, Germany

Received 2 November 2004; accepted 30 November 2004

Abstract

Multiple collector mass spectrometry has enabled significant advances in our understanding of geological, biological, nuclear, and physical processes in terrestrial and extra-terrestrial environments. The development of improved mass spectrometers and more efficient and universal ionization techniques is driven by the requirement to extract the highest quality information from the smallest amount of sample possible. Important milestones include the refinement of the variable multiple collector system, improvements in current amplifier technology to achieve ultimate precision and accuracy, increased abundance sensitivity, tailored ion optics using zoom optics and increased ion optical magnification to meet the special requirements of multiple collection, increased signal-to-noise using multiple ion counting devices, and the integration of a high efficiency ionization inductively coupled plasma source. New applications are on the horizon in many fields in addition to the geological and cosmological origins of high precision isotope ratio mass spectrometry. This is made possible by in situ sampling of samples at high spatial resolution using laser ablation techniques as well as online coupling of chromatographic devices to study elemental isotope effects in isolated molecular species. This paper describes and discusses the instrumental development of multiple collector isotope ratio technology and highlights some emerging applications.

Keywords: Multicollector isotope ratio mass spectrometry; Thermal ionization; Inductively coupled plasma

---

1. Introduction

Atomic weights are not constant in nature because the isotope abundances of many elements are altered as a result of biological, chemical, physical, and nuclear processes. Therefore, the interpretation of isotope abundance data can be used to determine the source(s) of elements in a system, to identify and understand processes that affect an element, and to determine the ages of rocks and minerals based on the accumulation of a radiogenic daughter product. In many cases, isotope abundance differences can be subtle (on the order parts per thousand or per million) and specialized instrumentation is required to measure fractional changes. Mass spectrometry (MS) is an ideal tool to measure these effects because of its capability to reveal isotopic information over a large dynamic range. Instrumental improvements resulting in higher precision isotope ratio measurements were often the key for progress in science. The demand for high accuracy and high sensitivity measurements motivated developments in ionization and inlet techniques, ion optical design, vacuum systems, and detector technology. Different types of ionization sources are employed, each tailored to the nature of the raw material and element of interest. Thermal ionization (TI) is used primarily for sensitive measurements of the alkali, earth alkali, and rare earth elements (REE). Because of the selectivity of the surface ionization mechanism, in favorable cases, it can produce ion beams with very high ionization yields ranging up to 10% or more with very low backgrounds. This makes the TI ion source an ideal tool for high precision measurements for certain elements. Electron impact (EI) sources have been employed for elements that are most eas-

---

[*] Corresponding author. Tel.: +1 403 220 3641; fax: +1 403 289 3331.
E-mail address: mwieser@ucalgary.ca (M.E. Wieser).

1387-3806/$ – see front matter © 2004 Elsevier B.V. All rights reserved.
doi:10.1016/j.ijms.2004.11.029

ily converted and analyzed as gaseous species (i.e., carbon and oxygen as CO_2 or sulfur as SO_2). Secondary ion mass spectrometry combined with ion microprobes has evolved as a powerful tool for in situ isotope ratio measurements at high spatial resolution. Inductively coupled plasma (ICP) ionization methods are opening entirely new applications of isotope measurements because of the sensitivity for all elements including those with high first ionization potentials (i.e., Fe and Hf), which are difficult to ionize with a TI source. Since the ICP source is an atmospheric pressure ionization source, the sample can be introduced directly at atmospheric pressure. There is great potential to combine on-line sample preparation devices with high precision isotope ratio mass spectrometry.

The return of samples from the Apollo Lunar missions of the 1960s and early 1970s motivated the development of advanced clean-room analytical procedures and high precision isotope ratio mass spectrometers. In the same way that the Lunar missions drove early developments in isotope ratio mass spectrometry, one of the motivations to advance high sensitivity high precision instrumentation today is the anticipated return of Martian mineral samples. However, the amount of Martian material will be a fraction of what was available from Lunar missions and will require instrumentation with significantly increased sensitivity and precision from much smaller amounts of sample. An area of intense investigation will be the search for isotope abundance ratio patterns that might indicate past biological activity in the Martian environment. Precision and accuracy of the measured isotope ratios are closely linked to the technology used. The scope of this paper is to discuss the limitations as well as the possibilities of current multiple collector instrumentation for challenging applications in different fields of research.

2. The magnetic sector mass analyzer

The most important feature of magnetic sector mass spectrometers, that is not available with other types of mass analyzers (including quadrupole, ion trap or time of flight mass spectrometers), is that the ion beams of different masses are spatially separated in the focal plane of the mass analyzer. This gives the unique possibility of setting up a multiple collector arrangement where one can position a separate detector for each isotope of interest for simultaneous detection. Another characteristic of the magnetic sector isotope ratio mass spectrometer is the combination of high mass resolution (i.e., $M/\Delta M = 10{,}000$) and "flat-topped" peaks. This ensures that the entire ion image produced in the source is incident on the detector and that small fluctuations in the position of the ion image in the focal plane do not result in variations in the measured ion current intensity.

The first magnetic sector mass spectrometers were equipped with a single Faraday cup detector. Isotopic ion currents were measured in a peak-jumping mode by varying the magnetic field strength or accelerating potential in the source. Because of the sequential measurement of different isotopes, the precision of the measured isotope abundance ratios were highly dependent on the stability of ion emission in the source and temporal drift algorithms were employed to compensate for smooth signal drifts. Under favorable conditions, precisions better than 50 ppm could be achieved. In general, the sensitivity of a single collector measurement is poor because the time spent measuring a given ion current is low relative to the duration of the entire measurement cycle.

2.1. Static multicollector instruments

In order to overcome the limitations of single collector mass spectrometers, multiple collector instruments capable of measuring several isotopic ion currents simultaneously were developed. Simultaneous collection improves the precision tremendously because small fluctuations in the ion beam affect the measurement of all ion current and most of the analysis time is spent measuring all ion currents. Smaller amounts of sample can be measured faster and with greater precision compared to single collector designs. Early commercial instruments offered by Finnigan MAT and VG isotopes had as many as nine Faraday cup detectors in a fixed configuration arranged for specific isotope systems. A given system might be configured to measure Pb isotopes, but could not be used to measure isotopes of Sr because the spacing between the ^{206}Pb, ^{207}Pb, and ^{208}Pb collectors is smaller than the spacing between the ^{86}Sr, ^{87}Sr, and ^{88}Sr. Galer and Spectromat [1] as well as NU Instruments [2] have come up with a multicollector instrument design with a fixed collector array but using zoom optics to change the mass dispersion of the ion optics. In this design, the mass dispersion (i.e., the spacing of the separated isotope ion beams along the focal plane) of the mass spectrometer is adjusted by ion optical means to fit into the fixed detector array. This procedure works well for measurements where low mass resolution is sufficient. If high mass resolution is required, then a variable and moveable slit system in front of each detector is desirable to enable fine adjustments of the detector slit positions to separate the elemental peak from the interferences.

2.2. Variable multicollector instruments

Another approach in multiple collector instruments was the development of variable multiple collector arrays where the positions of the individual Faraday cup detectors can be changed to accommodate different isotope systems. Because of its flexibility, variable multiple collector systems are regarded as the most universal multiple collector approach. The mechanical design has to be robust to withstand frequent adjustments, but still ensure that the detectors can be positioned with micrometer precision. This is particularly significant for the measurement of isotope ratios where molecular interferences need to be resolved from the elemental isotope peak by high mass resolution. For example, consider interferences that require a mass resolution of $R = M/\Delta M = 3000$ to be separated. Assuming a standard-sized sector field mass analyzer, the spacing of the two beams in the focal plane of the mass spectrometer is as small as ~0.2 mm and the detector positions need to be adjusted to better than ±20 μm to ensure a good peak overlap of several isotopes at the same time. Recent instrumental developments have further expanded the definition of variable multiple collection from simply varying the *position* of the collectors to include changing the *type of detector* as well. Specialized ion counters have been developed that are interchangeable with standard-sized Faraday cups (see Section 3.6).

3. Ion current measurement

3.1. Faraday cup detectors

The noise inherent in the Faraday cup detectors and associated electronic circuits is a limitation to the practical sensitivity of the measurement. State-of-the-art instrumentation uses Faraday cup detectors current amplifiers with high-ohmic resistors (typically on the order of 10^{11} Ω) in the feedback loop (Fig. 1a). The dominant source of noise is Johnson noise generated by the high ohmic resistor. Optimum operating conditions are achieved when the current amplifiers are maintained in an evacuated and temperature-stabilized housing. Typically, the temperature coefficients of the high-ohmic resistors are in the range of 200 ppm/°C. This means that the ambient temperature of the resistor must be kept stable to better than ± 0.01 °C if a gain stability of 2 ppm is required.

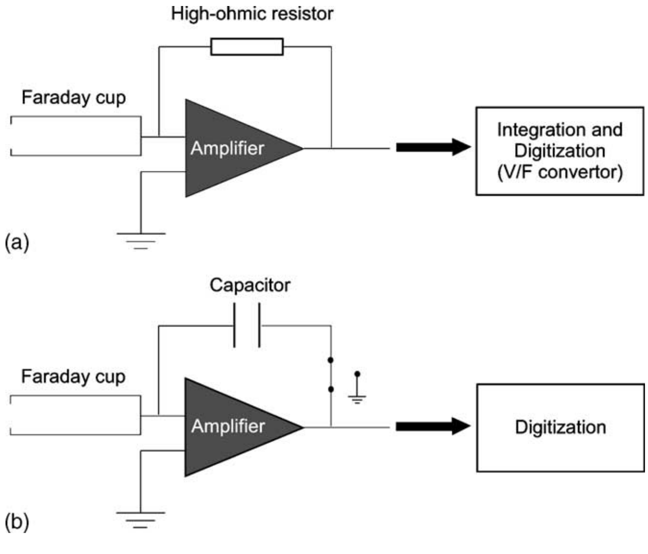

Fig. 1. The most commonly employed ion detection method is the Faraday cup detector. (a) Incoming charge can be converted to a voltage by an operational amplifier with a high-ohmic feedback resistor. (b) Substituting a capacitor for the high-ohmic resistor in the feedback loop of the operational amplifier results in a charge integrator avoiding the Johnson noise of the resistor.

The Johnson noise (ΔV) of a resistor is given by Eq. (1).

$$\Delta V = \sqrt{\frac{4k_\mathrm{B} RT}{t_\mathrm{m}}} \tag{1}$$

where k_B is Boltzmann's constant; R the resistor value in Ohms (Ω); T the temperature in Kelvin; t_m is the integration time.

From this equation, it can be seen that the noise amplitude scales with the square root of the integration time. If the integration time is increased by a factor of 4, then the noise is decreased by just a factor of 2. If a larger value feedback resistor is substituted in the amplifier, the gain of the amplifier increases linearly with the resistor value, while the noise level only scales with the square root of the resistor value. For instance, if the resistor value is increased by a factor of 10 (from 10^{11} to 10^{12} Ω), the relative noise level should improve by a factor of $\sqrt{10}$. However, in practice, the signal-to-noise improves only by a factor of 2 because parallel current pathways in the amplifier, the limited resistance of the vacuum feedthrough, and the insulation of the Faraday cup are comparable to the value of the feedback resistor and as a consequence the input noise of the operational amplifier itself is amplified and contributes to the noise amplitude (Fig. 2). Further increases in the value of the high-ohmic resistor to measure smaller ion currents encounter a practical limit to improvements in the signal-to-noise ratio.

In order to circumvent Johnson noise, a small capacitor can be substituted for the resistor in the feedback loop of the operational amplifier (Fig. 1b). This approach has been tested on a prototype developed by Esat [3] and the authors report that the noise level was reduced by a factor of 20. This is a significant advance for many applications. However, such a design demands perfect control of all leakage currents and the entire setup must be isolated with sapphire insulators. Special current amplifiers with extremely low and stable input bias currents in the range of 10^{-17}–10^{-18} A are needed. In addition, little is known about the linearity and stability of these devices and so far the capabilities of this concept have only been tested for very small signals.

3.2. Secondary electron multipliers

Electron multipliers are used to further extend the sensitivity of the instruments by several orders of magnitude, either in current amplification or ion-counting modes. These devices function by converting incoming ions into secondary electrons. With this type of detector, the greatest sources of uncertainty are dead time corrections, linearity, and dark noise [4]. The mode of operation depends on the magnitude of the high voltage applied to the device. If the electron multiplier is operated in a medium amplification range with a gain of 10^3–10^5, then the resulting current at the output of the electron multiplier can be measured in an analog mode using conventional low-current amplification techniques. A significant disadvantage for electron multipliers operated in the analog

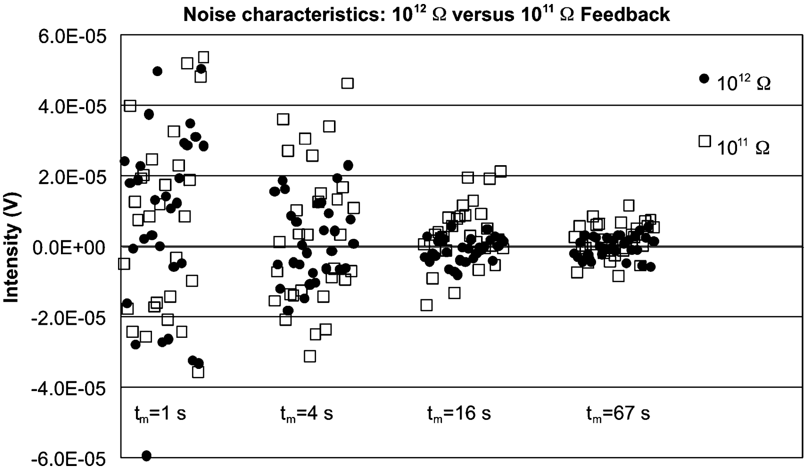

Fig. 2. The effect of the noise level with respect to different integration times and resistor values (10^{12} and 10^{11} Ω) is illustrated. The integration time between the different groups of data points is scaled by a factor of 4 and the spread of the measured data points is reduced by a factor of 2. The spread of the data using 10^{12} Ω resistor is about two times smaller compared to the data using 10^{11} Ω resistor. The different gains due to the different resistor values have been considered.

mode is the fact that the number of secondary electrons produced at the first conversion dynode depends on the impact momentum of the incoming ion and the statistical nature of electron amplification along the dynode structure. Thus, for monoenergetic ions, the amplification is mass dependent. A consequence is that the electron multiplier will cause a systematic offset in the measured isotope abundance ratio when used in analog mode. In addition, any charging effect inside the discrete dynode structure can result in a significant nonlinearity in the output current as a function of different signal intensities.

At higher amplification in the range of 10^6–10^8, the gain is large enough that individual electron pulses can be readily detected and counted using sensitive pulse counting electronics (Fig. 3). This mode of operation of the electron multiplier is known as ion counting. All ion pulses greater than a certain threshold level are counted. In this mode of operation, the measured intensity (i.e., the number of pulses) is much less dependent on the amplification process of the dynode structure since the actual height of the individual pulses is no longer considered. Pulses are counted as long as they are greater than the threshold voltage, which is typically in the range of 2–5 mV. Ion counting detectors offer high sensitivity and mass dependent detection efficiencies are greatly reduced and can be neglected. This design works efficiently for negative and positive ion detection.

A special detector described by Daly [5] was based on a three-step conversion process. First, incident positive ions are accelerated onto a polished aluminum knob held at high negative potential (Fig. 4). Because of the high impact momentum of the ions on the conversion knob, a large number of secondary electrons are released (first step). These electrons are subsequently attracted by a scintillator screen held at ground potential. When the high-energy electrons hit the scintillation screen, a portion of the energy of the electrons is converted into photons (second step), which are finally detected by a photomultiplier (third step). The photomultiplier and detection electronics are held at ground potential. This technology is best employed for positive ion detection. If negative ions are to be measured, the acceleration voltage at the first conversion knob has to be positive and since the secondary electrons must be further accelerated to the scin-

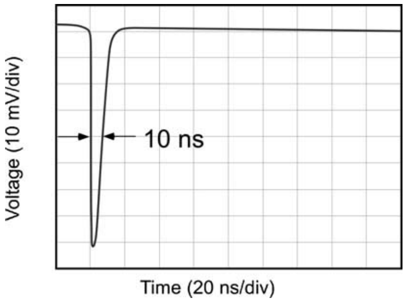

Fig. 3. A typical output pulse of an electron multiplier operated in ion counting mode. The full width half maximum (FWHM) of the pulse is less than 10 ns and the amplitude can be as high as 100 mV. Typically the pulse height is in the range of about 50 mV.

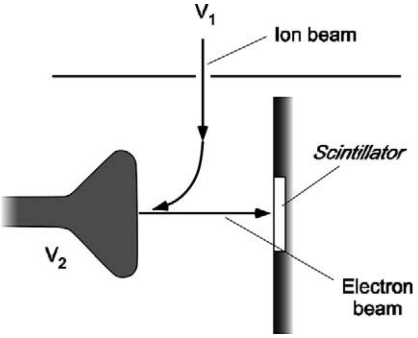

Fig. 4. The Daly detector converts incoming ions to electrons, which are accelerated to a scintillator where they generate light pulses that are finally detected by a photomultiplier detector (modified from [5]).

tillation screen the potential of the scintillation screen has to be at even higher positive voltages and can no longer be maintained at ground potential. This results in a region with very high electrical field strengths close to the sensitive ion counting detector. As a consequence, in practice there is a high susceptibility for noise. Typically, Daly detectors are used for positive ion detection only.

3.3. Abundance sensitivity: high dynamic range isotope ratio measurements

The actual ratio and terrestrial variation in ^{232}Th/^{230}Th is large, and for some samples the ratio is in the range of 140,000–300,000. The measurement of ^{233}U/^{238}U and ^{236}U/^{238}U isotope abundance ratios can be employed to study nuclear fission reactions, where the ratios may be in the order of a 1:500,000 or even smaller. The measurement of isotope ratios covering this large dynamic range requires clean backgrounds in the mass spectrum. Interferences must be avoided by clean sample preparation and also scattering of the ions along their way from the entrance slit to the detector slit have to be minimized. Ions colliding with residual gas molecules along the ion optical flight path and/or scattering on edges of the beam defining apertures will lose energy and/or slightly change their ion optical trajectory. As a consequence these scattered ions will appear at a different position in the mass spectrum. The magnetic sector deflects ions with reduced ion energy with a smaller radius and thus scattered ions preferably build up a tail on the low mass side of the major peak. In extreme cases, the tail of the higher mass ions can completely cover the peak of a minor isotope in the mass spectrum so that even the detection of the minor isotopes would be impossible. In order to minimize scattering along the ion optical path, an ultra-high vacuum inside the mass analyzer is important and sharp edges on any aperture in the mass spectrometer are advantageous. In general, the abundance sensitivity of the mass spectrometer is specified as the relative intensity of the spectral background signal measured at one mass unit spacing on the low mass side of an intense isotopic ion current. Usually the abundance sensitivity is measured at mass 237 in the presence of an intense ^{238}U beam. Typically, the vacuum inside the mass analyzer should be maintained at better than 10^{-8} mbar. Thus, instruments should be constructed from stainless steel and all-metal gaskets to ensure a leak-tight vacuum region and to enable the analyzer to be heated to >120 °C to drive off adsorbed gases and water vapour. The abundance sensitivity for state of the art multiple collector instruments is typically in the range of 1–5 ppm.

In order to further improve the abundance sensitivity, an early approach was to combine two first order single focusing magnetic sectors in an “S” configuration [6]. This design realized improvements in abundance sensitivity by a factor of 1000 over single magnetic sector instruments. However, the combination of two magnetic sectors resulted in a large and complex instrument that, while offering improved abundance sensitivity, did not offer higher mass resolution over single sector designs.

Adopting the strategy of multiple sectors to reduce the scattered background in sector instruments, the VG ISOLAB-120 [7] was designed to measure ^{9}Be/^{10}Be isotope abundance ratios, which are on the order of 10^9 in natural materials (Fig. 5). An electrostatic analyzer (ESA) is placed in front of the entrance to the ion counting detector and a fixed potential difference is applied to the two curved plates of the ESA such that only ions with a specific kinetic energy can emerge. A similar approach was incorporated into the VG Elemental Sector 54. Here, a 30 cm radius electrostatic sector with energy filtering characteristics was installed prior to a Faraday cup and Daly detector. This resulted in an improvement in abundance sensitivity of about a factor of 10.

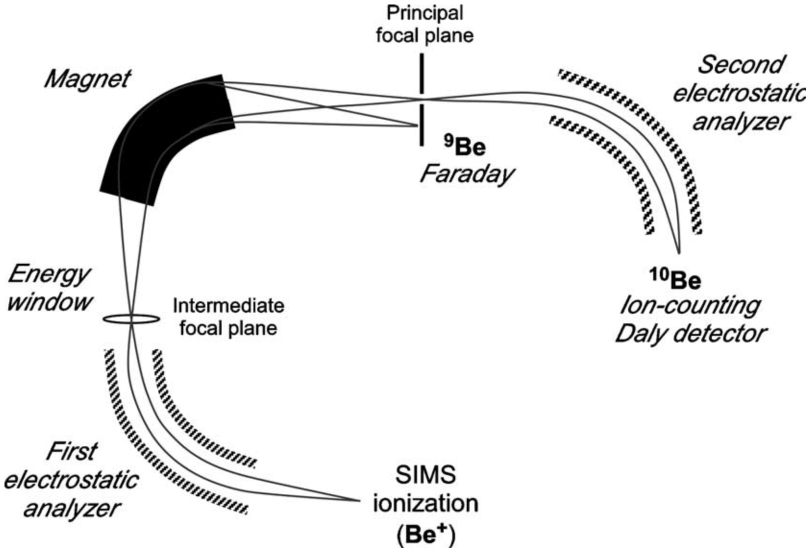

Fig. 5. The VG ISOLAB 120 mass spectrometer used an electrostatic analyzer prior to the entrance of an ion counting detector to achieve high abundance sensitivity (modified from [7]).

Freeman et al. [8] describe a different strategy. They used a gridded (600 mesh copper) retardation lens situated after the final exit slit of a magnetic sector mass spectrometer. A variable bias of ±150 V on top of the accelerating voltage was applied to the gridded retardation lens such that only ions above certain energy were transmitted to the detector. An increase in abundance sensitivity by a factor of 10 from $\sim 10^4$ to $\sim 10^5$ was achieved.

Following the approach using a retardation lens, the Finnigan MAT262 employed the retarding potential quadrupole (RPQ) lens prior to the axial ion counter to improve abundance sensitivity (Fig. 6). The RPQ had no grids and incorporated special beam shaping quadrupole lenses to ensure good peak flatness [9,10]. Combined with a TI source, this device achieved an improvement in abundance sensitivity of two orders of magnitude from 2 ppm to 20 ppb. The RPQ lens acts as an energy filter to discriminate against ions that have lost some energy due to scattering events (either collisions with residual gas particles or apertures within the analyzer). Since it is an ion optical lens, it also is sensitive to ions that have slightly changed their fight directions and ions with perturbed trajectories will be discriminated by the retardation lens as well. Since the energy distribution of the ions generated in a TI-MS source is very narrow, i.e., ≤1 eV, a very sharp cut-off in the transmission curve of the RPQ can be observed as the suppressor lens voltage is increased. The optimum working point is close to the knee in the transmission curve. At this point the abundance sensitivity is ∼20 ppb while the transmission is close to 100% (Fig. 7). In case of an ICP ion source, the energy spread of the ions is much greater. For instance, with a shielded torch, the energy spread of the ICP ions is about 5 eV and as a consequence the cut-off in the transmission curve is extended over a range of the suppressor voltage of 7 V. The abundance sensitivity improvement by the retardation lens is about a factor of 10 better on a TI-MS compared to the ICP-MS. This is related to the much sharper cut-off characteristics of the transmission curve in case of TI-MS. (Fig. 7). For some special applications, and depending on the emission characteristics of the ion source, much higher abundance sensitivities can be achieved. Lee et al. employed the RPQ on a MAT262 with an abundance sensitivity of 10^{-11} at two mass unit spacing to measure ^{135}Cs/^{133}Cs

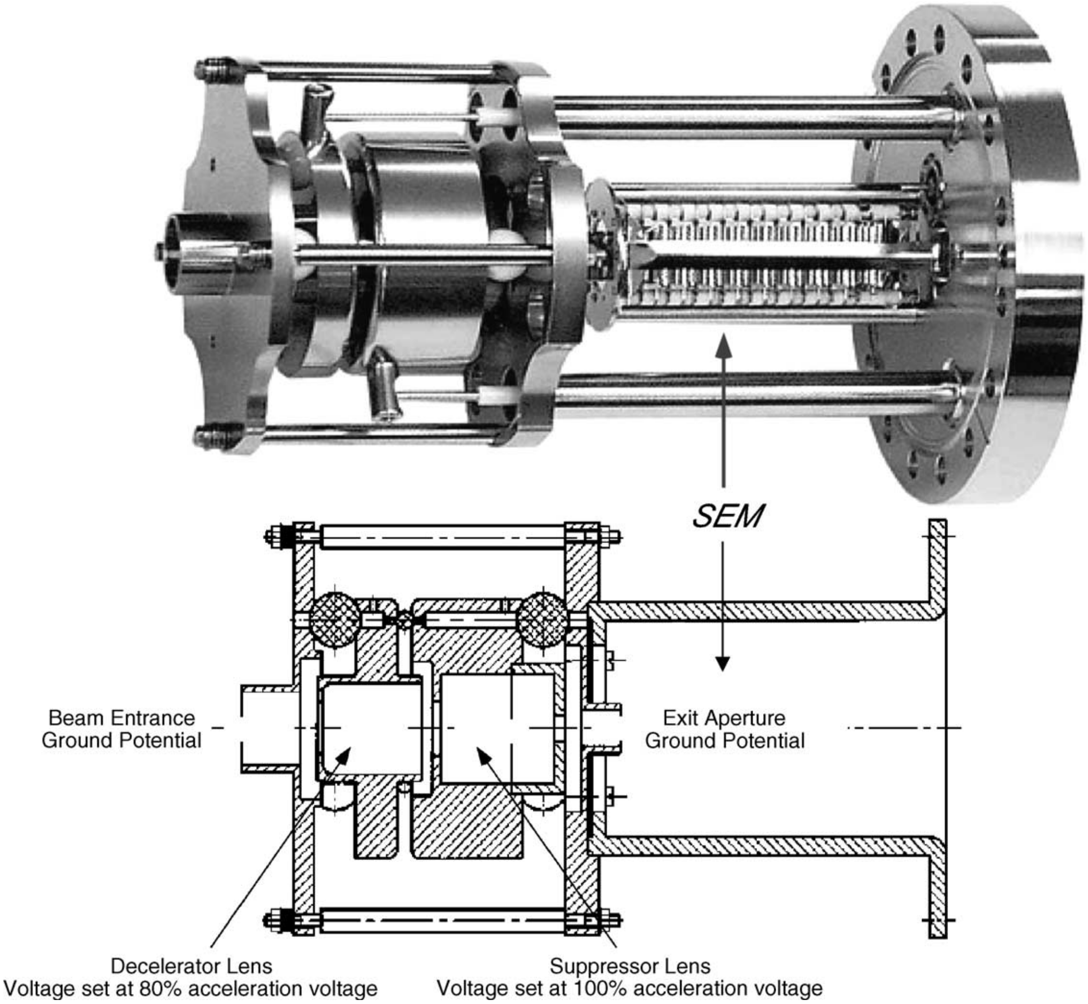

Fig. 6. RPQ lens used in the Finnigan TRITON and Finnigan NEPTUNE.

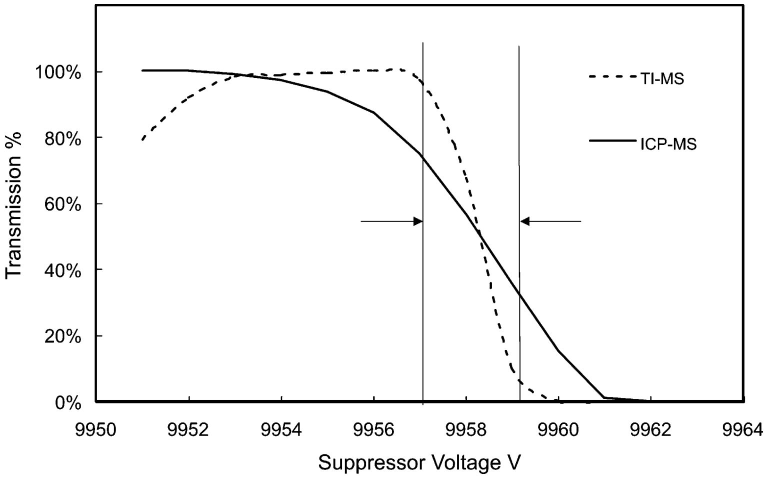

Fig. 7. The transmission curve of the RPQ retardation lens for TI-MS (Finnigan TRITON) and ICP-MS (Finnigan NEPTUNE). Due to the smaller energy spread of the ions, the curve for TI-MS is much sharper.

ratios to search for ^{135}Cs from fallout in coastal sediments [11].

3.4. Accuracy and precision of dynamic multiple collection measurements

Common to all multicollector systems is the need to cross-calibrate the detector gains against each other to account for the individual response of each device. Typically, the gain calibration factors of the current amplifiers used for the Faraday cup detectors are measured by connecting the inputs of the current amplifiers sequentially to a stable reference current and measure the response of the current amplifier. The ratios of the measured signals are the electronic cross calibration factors, respectively, the electronic gain calibration factors of the detector channels. This is not needed for single collector instruments because all signals are measured on the same detector and the gain factor is cancelled by the calculation of the isotope ratio. The accuracy of the isotope abundance ratio measurement also depends on a linear response of the detector over a large dynamic range and the cup efficiency, sometimes referred to as cup factors.

Cup efficiencies are more difficult to account for because these depend on the Faraday cup itself including the material used and geometry of the detector. Calibration of cup efficiencies requires that ion beams are incident at the entrance of the Faraday cup. Ideally, the cup efficiencies would all be identical. But, since these detectors are exposed to ion beams, some radiation damage of the surfaces may result in non-uniform behavior of the Faraday cups. For instance, insulating surfaces may accumulate inside the Faraday cup and surface charge can accumulate and the response of the cup will change over time. A workaround to eliminate different cup efficiencies is to use a “multi-dynamic” measurement strategy such that cup factors cancel out [12,13]. For example, consider the measurement of ^{86}Sr, ^{87}Sr, and ^{88}Sr using two collectors. A two-line measurement is designed as shown in Table 1. The ^{87}Sr/^{86}Sr isotope abundance ratios are then calculated as shown in Eq. (2):

$$\frac{^{87}\mathrm{Sr}}{^{86}\mathrm{Sr}}_{\mathrm{MD}} = \sqrt{\left(\frac{^{87}\mathrm{Sr}}{^{88}\mathrm{Sr}}\right)_{\mathrm{Line1}}\left(\frac{^{87}\mathrm{Sr}}{^{86}\mathrm{Sr}}\right)_{\mathrm{Line2}}\left(\frac{^{88}\mathrm{Sr}}{^{86}\mathrm{Sr}}\right)_{\mathrm{Norm}}} \quad (2)$$

The first and second terms are both static measurements and the ratio must be corrected for the cup factors only and not temporal drift. Note, however, that the first ratio includes the ratio of the cup factors for collector #2 to #1 and the second term contains the ratio of the factors for collector #1 to #2. Therefore, these factors cancel and there is no need to measure them independently. The calculation also includes a correction for mass dependent fractionation based on an accepted ^{88}Sr/^{86}Sr isotope abundance ratio.

3.4.1. Using zoom optics to change mass dispersion

The dispersion or separation distance between masses in the focal plane depends on the relative mass difference of the ions. While one can position two collectors to achieve perfect peak overlap for one pair of isotopes (i.e., either for ^{87}Sr and ^{86}Sr or ^{88}Sr and ^{87}Sr), at least one isotope from the other pair will strike another point of the detector (Fig. 8) possibly resulting in different cup efficiencies so that the gain ratios are not necessarily cancelled in Eq. (2). Zoom optics integrated into the mass analyzer enable the dispersion to be changed so that perfect peak overlap is achieved for all configurations used in the multidynamic sequence. When used synchronously while switching between the isotope pairs, the zoom optics can enhance the performance of multidynamic measurements. But, even with the support of zoom

Table 1
A two-line multi-dynamic measurement sequence for strontium

Line	Collector #1	Collector #2
1	^{88}Sr	^{87}Sr
2	^{87}Sr	^{86}Sr

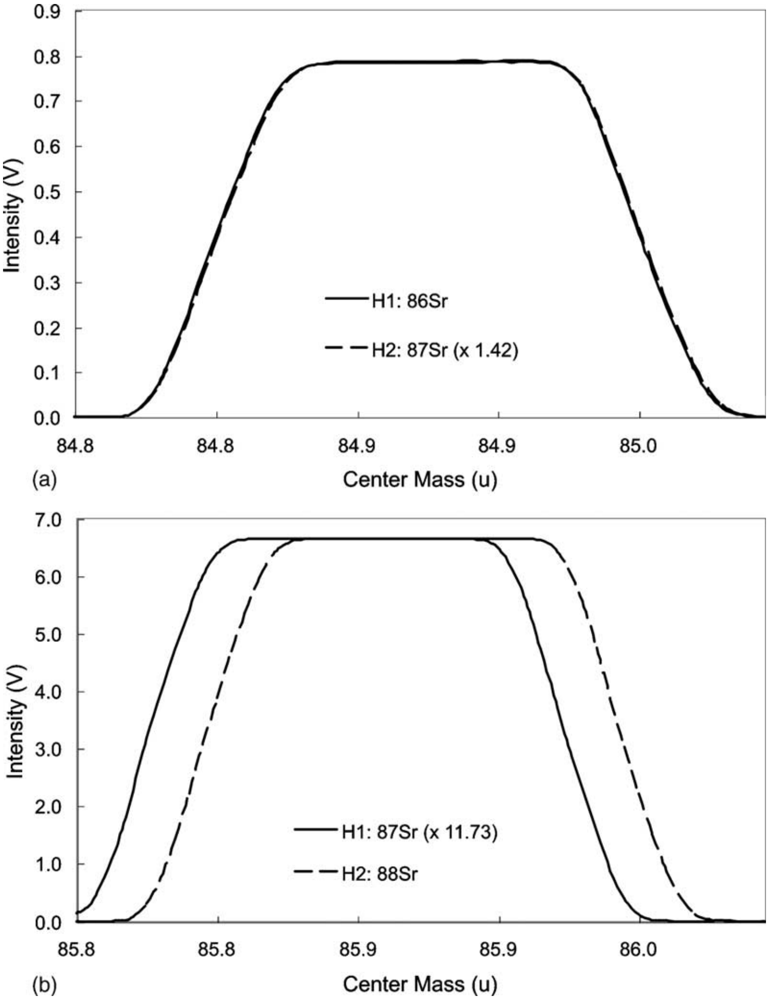

Fig. 8. (a) Mass scan showing optimum peak overlap of masses ^{86}Sr and ^{87}Sr. The cups have been mechanically adjusted to achieve optimum peak overlap. Trace ^{87}Sr has been normalized to the same intensity as trace ^{86}Sr. (b) Mass scan showing mismatch of peak overlap of ^{87}Sr and ^{88}Sr measured in the same cups with the same spacing as (a).

optics, the multi-dynamic procedure remains a workaround to circumvent instrumental limitations. The ultimate goal of further instrumental developments should be to completely avoid changing cup efficiencies.

3.5. *The limits of static multiple collection*

The static multicollector measurement strategy should result in the highest precision in the shortest amount of time. This requires that the Faraday detectors as well as the current amplifiers are stable and linear. Through careful selection of materials, sophisticated cup design and purpose-designed ion optics, the performance of the Faraday cup can be improved. For instance, in order to enhance the operation of the Faraday cup, it is advantageous to increase the ion optical magnification of the multiple collector ion optics. Unlike systems that aim for stigmatic focusing with an overall ion optical magnification close to unity, the multiple collector platform of the Finnigan TRITON and NEPTUNE employ an optical magnification of $M = 2$ (Fig. 9). This results in a larger layout of the instrument, and results in improved Faraday cup performance (Fig. 10). The Faraday cups can be made twice as wide since the mass dispersion scales linearly with the ion optical magnification. The angular divergence of the ion beam at the detector is linearly reduced as the ion optical magnification is increased. As a consequence, the effective depth at which the ions start to strike the side walls of the Faraday cup is significantly increased as well. Thus, it is less likely that secondary particles generated inside the Faraday cup can escape and alter the measured ion current. Both, the larger width and the larger depth of the cups improve the performance of the Faraday cups.

Even if the performance of the Faraday cups is improved, there are still limitations with respect to the cross calibration of the current amplifiers. With a state of the art measurement system, the reproducibility of the electronic cross calibration of the amplifier gains is about 5 ppm (1 R.S.D.). For the measurement of an isotope ratio, at least two measurement channels are involved and the calibration factor of each channel is uncertain by 5 ppm. Thus, the resulting uncertainty for the

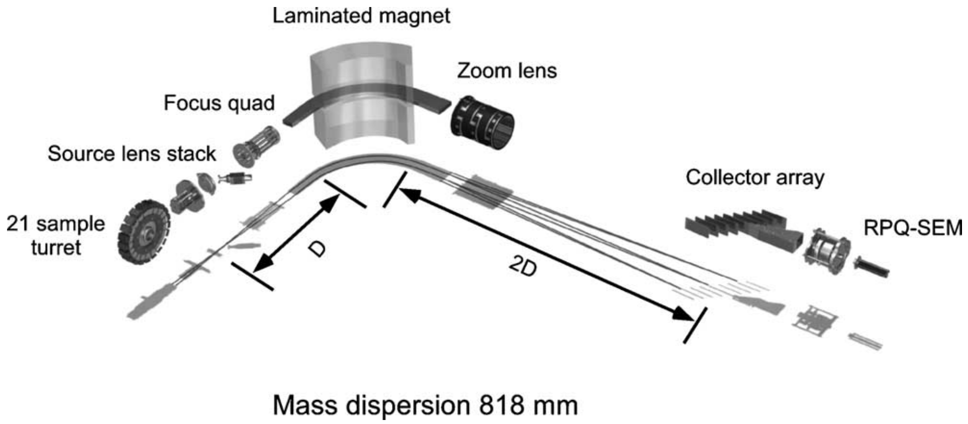

Fig. 9. Layout of the Finnigan TRITON TI-MS ion optics.

external reproducibility of multiple collector measurements can never be better than Δ as shown in Eq. (3):

$$\Delta = \sqrt{(5\text{ppm})^2 + (5\text{ppm})^2} \approx 7\text{ppm} \tag{3}$$

This means that the ultimate reproducibility of static isotope ratio measurements is limited to about 7 ppm (1 R.S.D.) at best and is due to the inherent uncertainty of the gain calibration procedure. This problem must be solved if a higher level of precision is required. The “Virtual Amplifier” design on the Finnigan NEPTUNE and TRITON seeks to eliminate the bias caused by uncertainties in the gain calibration of the amplifiers [14] (Fig. 11). Unlike classical multiple collector current amplifier systems, the Virtual Amplifier does not use a fixed connection between the Faraday cup channels and the current amplifiers. By means of a relay matrix, it is possible to setup the system such that amplifiers are switched between different Faraday cups during the measurement.

In order to explain the principle of the Virtual Amplifier concept, assume that there are just two isotopes to be measured: Iso1 and Iso2. Iso1 is measured in Faraday cup A and Iso2 is measured in Faraday cup B. In the Virtual Amplifier mode, the measurement is made in two blocks. In the first block, amplifier A is connected to Faraday cup A and amplifier B is connected to amplifier B. In the second block, the amplifiers are switched between the cups so that now amplifier A is connected to Faraday cup B and amplifier B is connected to Faraday cup A. Further, assume that amplifier A and amplifier B have both passed an electronic gain calibration procedure. Since the reproducibility of the gain calibration is limited to about 5 ppm each, it could happen that the calibration factor of amplifier A has been determined 5 ppm too high and that at the same time the calibration factor of amplifier B has been determined to be 5 ppm too low. In this case the measured ratio in the first block would be calculated as shown in Eq. (4).

$$\frac{\text{Iso1}_{\text{measured}}}{\text{Iso2}_{\text{measured}}} = \frac{\text{Iso1}_{\text{true}} \times \text{Gain(A)}}{\text{Iso2}_{\text{true}} \times \text{Gain(B)}} = \frac{\text{Iso1}_{\text{true}}}{\text{Iso2}_{\text{true}}} \times 1.00001 \tag{4}$$

This means the measured and gain corrected isotope ratio of the first block is systematically 10 ppm too high. However, in the second block, the amplifiers A and B are switched between the cups and measured isotope ratio calculates as given by Eq. (5):

$$\frac{\text{Iso1}_{\text{measured}}}{\text{Iso2}_{\text{measured}}} = \frac{\text{Iso1}_{\text{true}} \times \text{Gain(B)}}{\text{Iso2}_{\text{true}} \times \text{Gain(A)}} = \frac{\text{Iso1}_{\text{true}}}{\text{Iso2}_{\text{true}}} \times 0.999990 \tag{5}$$

The measured and gain corrected isotope ratio of the second block turns out to be systematically 10 ppm too low. However, the calculated run average of *both* blocks is accurate and the gain uncertainty is eliminated. This procedure also works as well for isotope systems with more than two isotopes. Following this concept, virtually all isotopes are measured with the same set of amplifiers and any gain uncertainty is systematically cancelled. The virtual amplifier approach is the key to break the 7 ppm external precision barrier of static multicollector measurements. For example, a significant question in the geological community is whether the mantle of the early Earth experienced a major stage of differentiation. The radiogenic decay of ^{146}Sm to ^{142}Nd is proving to be a promising, albeit controversial, isotope system to employ in

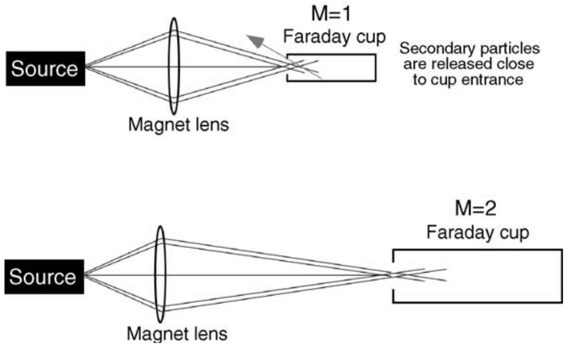

Fig. 10. The larger magnification of the ion optics results into a de-magnified angular divergence of the ion beam in the focal plane. As a consequence the ion beam enters deeper into the Faraday cups and is more safely captured by the Faraday cup.

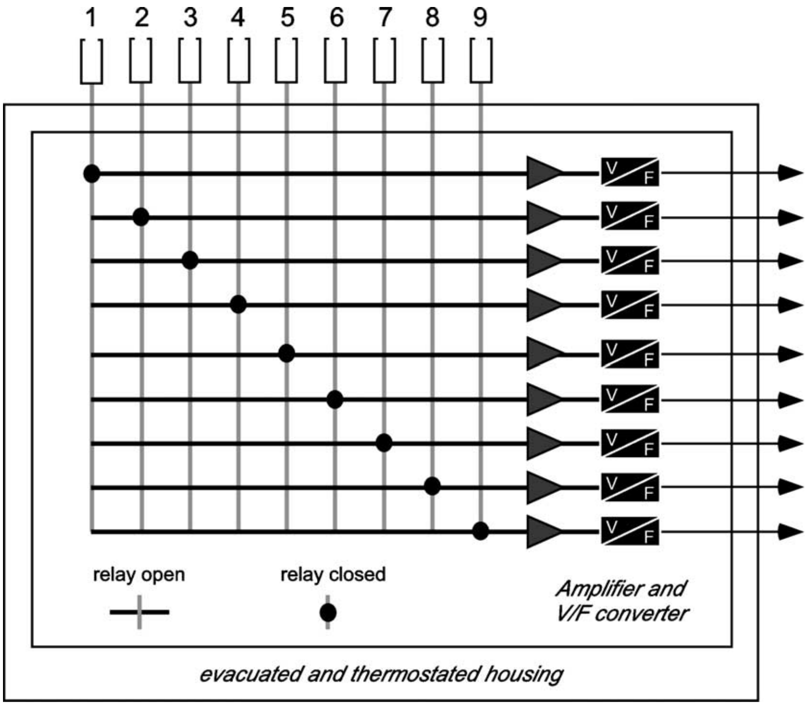

Fig. 11. The Virtual Amplifier used in the Finnigan TRITON and NEPTUNE. The amplifiers can be switched between different Faraday cups by means of a relay matrix.

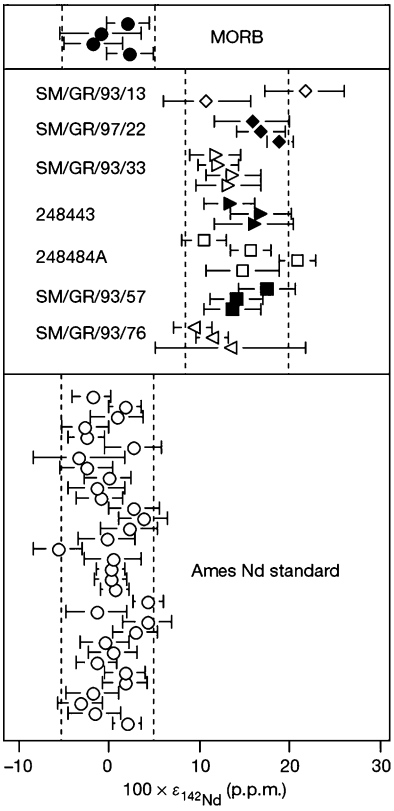

Fig. 12. ^{142}Nd anomalies resulting from the decay of ^{146}Sm detected in metamorphosed sedimentary rocks from Isua, Greenland [17]. The ^{142}Nd excess could be clearly identified because of the long-term reproducibility of the method, which was determined by replicate measurements of the Ames Nd isotope standard. Figure reproduced by permission from *Nature*.

the search for evidence of mantle subduction as recorded in Archean minerals. The half-life of ^{146}Sm is relatively short (103 Myr) and this radiogenic parent is now extinct. Therefore, anomalous amounts of ^{142}Nd in ancient rocks require that ^{146}Sm was common and suggest that the Earth's early crust must have formed before the planet was 100 million years old. Measurements of ^{142}Nd produced from the decay of ^{146}Sm are challenging because of the low initial abundance of the parent isotope. Thus, analytical techniques capable of extreme precision and sensitivity are required. Harper and Jacobsen [15] were the first to report excess ^{142}Nd in a 3.8 Ga Isua supracrustal from Greenland, which they associated with ^{146}Sm present in the parent material. These data were controversial and it was suggested that the small ^{142}Nd anomalies could not be resolved with mass spectrometers available at that time. Sharma et al. [16] later confirmed the ^{142}Nd anomaly, but noted that instrumental effects, including ion source focus and cup efficiencies, could result in long-term drifts that were on the same order as the ^{142}Nd anomaly. Recently, Caro et al. [17] used the Finnigan TRITON thermal ionization mass spectrometer with the virtual amplifier concept and static measurements to resolve ^{142}Nd anomalies of 15 ± 4 ppm (2σ) in metamorphosed sedimentary rocks from Isua, Greenland, measured relative to a Nd standard (Fig. 12). The authors could confidently identify this excess because of the long-term external reproducibility of 5 ppm (2σ). Caro et al. [17] used an exponential law to correct for mass fractionation during analysis followed by a second normalization to account for, what the authors describe as, non-ideal mass fractionation of unknown origin. Caro et al. have since reported

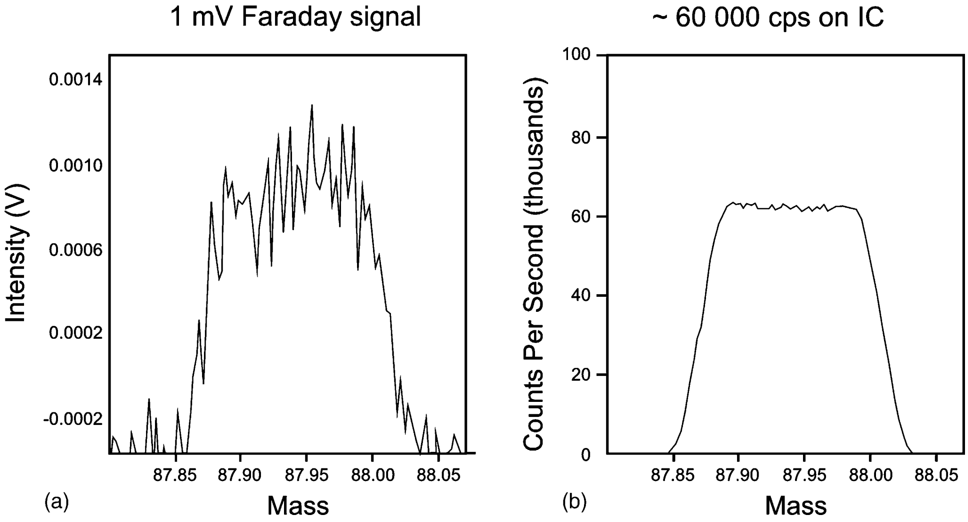

Fig. 13. Ion beam of the same intensity (a) scanned across a Faraday cup and (b) an ion counting detector. The improvement in the relative noise of the signal can be seen.

high levels of precision to better than 2 ppm (2σ) without the need for a second normalization [18].

3.6. Multiple ion counting

New levels of sensitivity are being realized by incorporating multiple ion counters in the detector array. This combines the most significant advantages of multiple collection, namely immunity to fluctuations in ionization and efficient utilization of the ion current with the extreme detection power of ion counting (Fig. 13). Multiple ion counting (MIC) offers high detection power because the signal-to-noise ratio of an ion counter is much greater than that of the Faraday cup detector; the noise of the ion counter arising primarily from dark noise and dead time, linearity effects, and finally counting statistics. Different manufacturers have introduced different configurations. GV Instruments developed a multiple ion counting system with conversion dynodes and compact Channeltron type detectors. NU Instruments uses conventional discrete dynode multipliers. In the NU Instruments analyzer, a maximum of three ion counters may be installed. The Finnigan TRITON and NEPTUNE employ miniaturized ion counting devices that are identical in size and interchangeable with standard Faraday cup detectors. This multiple collector can be configured with as many as nine Faraday cup detectors and eight miniature ion counters (Fig. 14).

The high detection power offered by multiple ion counting is essential for many applications where the amount of sample is limited, the dynamic range of several isotopes is very large and the signal is transient and therefore decays too rapidly to be measured with a single collector in a peak-jumping sequence. For example, nuclear safeguard programs seek to determine the U isotope abundances of individual micron size particles. Anomalous amounts of ^{233}U, ^{235}U or ^{236}U may indicate that artificial isotope enrichment or depletion processes were the source of these particles. This application not only demands extreme sensitivity, but also high accuracy and reliability. In one experiment, five multiple ion counters in a Finnigan TRITON were arranged to collect ^{233}U, ^{234}U, ^{235}U, ^{236}U, and ^{238}U. The data from one 10-μm-sized UO_2 reference particle are shown in Fig. 15 [19].

Fig. 14. Multiple collector array from the Finnigan TRITON and NEPTUNE. Miniaturized ion counters identical in size to Faraday detectors are mounted on the high mass side (for U) and low mass side (for Pb). Connections to the miniaturized ion counters are completely independent from the Faraday cup signal lines protecting the integrity of the signals.

4. Inductively coupled plasma ion sources

The integration of an inductively coupled plasma source with the multiple collector platform by Walder and Freedman [20] initiated a completely new field of instrumental development. It combined the versatility of an ICP source with the experience the community had gained over time with the use of multiple collector instruments for TI-MS. The ICP

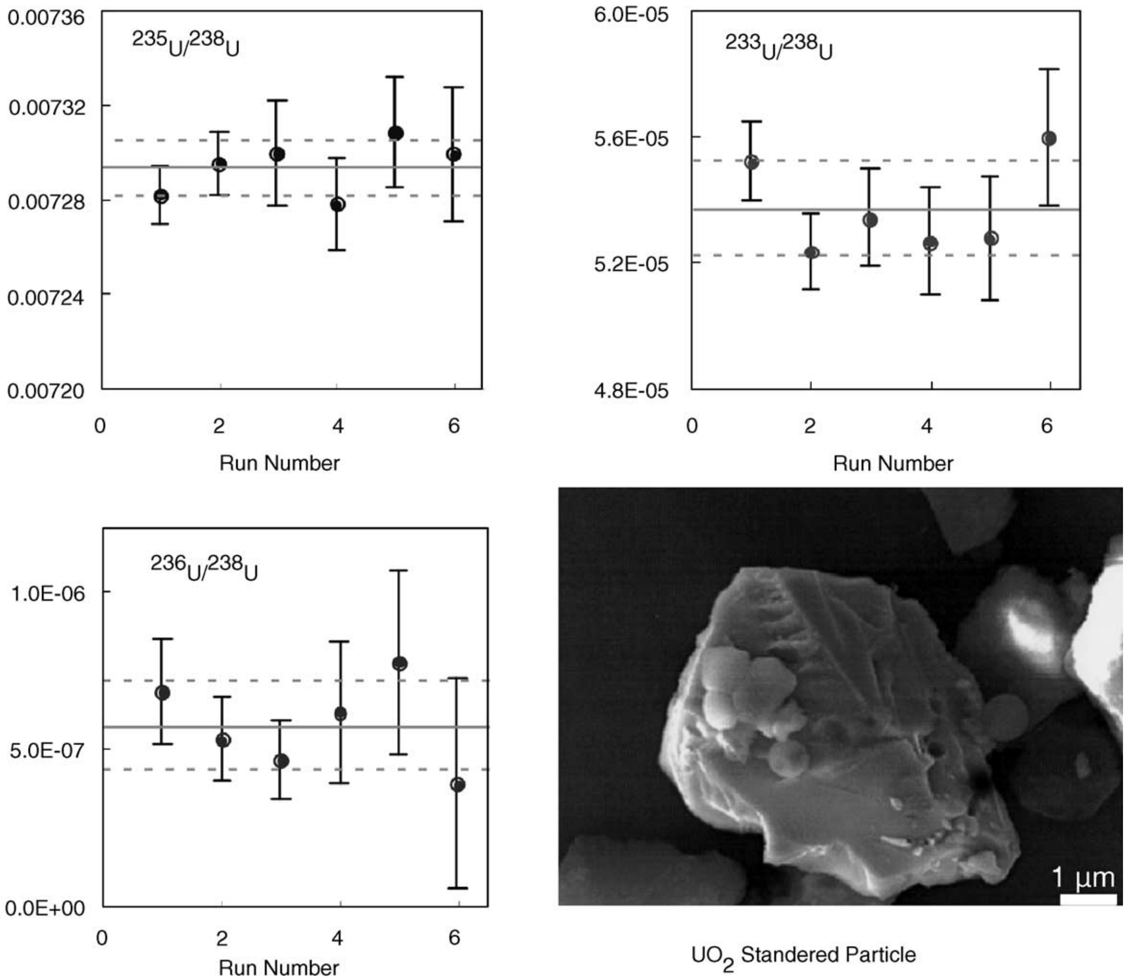

UO_2 Standered Particle

Fig. 15. U isotope abundance data from a single uranium oxide particle measured using multiple ion counters in a Finnigan TRITON. The high detection power of the multiple ion counter array was employed to search for anomalous $^{233}U/^{238}U$ and $^{236}U/^{238}U$ isotope abundance ratios. All errors are within counting statistics. The ^{238}U count rate decreased steadily from 70,000 cps to 15,000 cps over the six runs. Each run lasted 15 min. The measured $^{236}U/^{238}U$ isotope abundance ratios are on the same order as the abundance sensitivity at two mass units spacing and are at the limits of detection. If higher abundance sensitivities are required, one must employ an energy filter as described in Section 3.3.

source operates by inductively coupling a radio frequency (RF) field to a stream of Ar gas. The energy transferred to the Ar is sufficient to completely ionize the gas and create a high temperature plasma. This method can ionize elements with high first ionization potentials more efficiently and for some elements like Hf it offers higher detection limits relative to thermal ionization sources. Multiple collection of all isotopes effectively averages the "flicker" noise induced in the ion beam by the plasma. The first commercially available multiple collector inductively coupled plasma mass spectrometer (MC-ICP-MS) was the Plasma 54 marketed by VG Elemental (Fig. 16). This instrument incorporated the analyzer platform of the Sector 54 thermal ionization mass spectrometer, which was modified to include an electrostatic analyzer prior to the magnetic field for energy focusing of the ion beam. The electrostatic sector was required for energy focusing because the energy spread of the ions produced in the plasma source was much greater than that observed in the TI source (∼25 eV compared with ∼2 eV). Nine Faraday cup collectors and a single Daly detector for ion counting were available.

Compared to TI-MS in particular, the high ionization efficiency and simplified sample preparation using the MC-ICP-MS caused a lot of excitement. It opened the possibility to analyze novel isotopic systems with ease and precision. It was even discussed whether MC-ICP-MS would render TI-MS obsolete because of the higher precision possible and simplified sample preparation and introduction. However, it is now accepted that very high precision requires careful sample preparation when using either ionization method. TI-MS and MC-ICP-MS are regarded to be complementary techniques that individually offer particular analytical strengths [21].

4.1. Isobaric interferences and the application of sector field mass spectrometers

Similar to TI-MS instruments, the first generation of MC-ICP mass spectrometers were designed with low mass resolu-

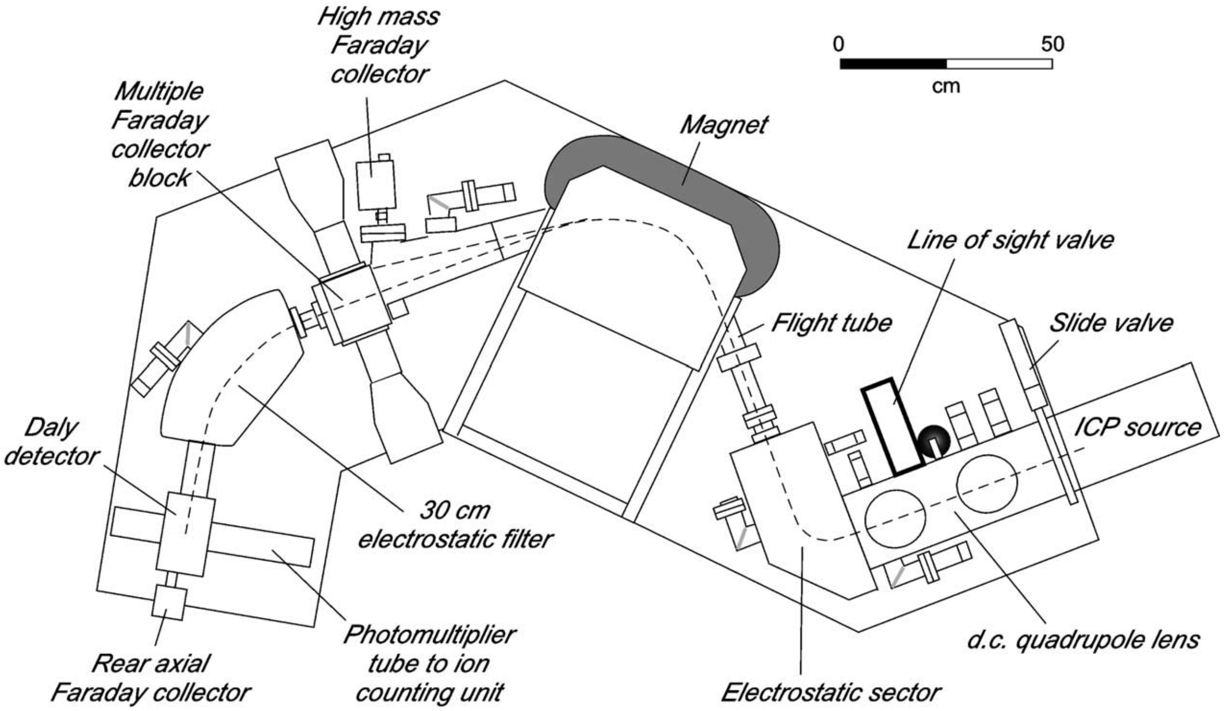

Fig. 16. The VG Elemental Plasma 54 was the first instrument to combine the versatility and high ionization efficiency of an ICP source with a multicollector platform designed for isotope abundance measurements.

tion ion optics. However, as interest grew in exploring stable isotope systems including Fe, Ca, Si, and Mg, the need for high mass resolution became unavoidable. High precision isotope ratio measurements require stable backgrounds and complete suppression of interferences. Ion-molecule interactions in the ICP source produce molecular interferences that may constitute serious isobaric interferences for the isotopic ion species of interest. In addition, trace amounts of contaminant elements can also interfere with the minor isotopes of the element being measured. For example, in the case of calcium isotope measurements, Sr^{++}, Ti^{+}, Ar^{+}, and hydrides of Ar and N appear at almost every Ca isotope (Table 2.)

High mass resolution through optical peak separation is the most universal and robust way to eliminate spectral interferences and the Finnigan NEPTUNE MC-ICP-MS was the first routine isotope ratio instrument designed specifically for high mass resolution. The Nu-1700 from NU Instruments is a large geometry double-focusing multiple collector ICP mass spectrometer designed for isotope ratio measurements at high mass resolution. It has an oversized geometry in order to achieve high mass resolution with high transmission. This instrument has a 943 mm radius 70° electrostatic analyzer followed by a 750 mm 70° magnetic sector.

In practice, high mass resolution that preserves flat-topped peaks is realized by adjusting the source slit to generate an interference-free space between ion beams in the focal plane of the mass spectrometer. The slits at the detector are set wider than the beam profiles in the focal plane. Selecting a wide detector slit width ensures a wide plateau as the ion beam is scanned across the focal plane. If the opening at the detector is wider than the distance between the two ion beams, the peaks will appear unresolved in a mass scan. Because of an isotope's mass defect, the polyatomic interferences in the low and medium mass range always occur on the high mass side of the elemental peaks, and as a consequence the location of the individual collectors in the multiple collector array can be positioned such that only the elemental isotopic ion currents are measured and the polyatomic interferences do not enter the detectors (Fig. 17).

Table 2
Elemental and molecular isobaric interferences affecting the measurement of calcium isotopes

Isotope	Natural abundance (%)	Interferences	Resolution required
^{40}Ca	96.941	$^{40}Ar^{+}$	192500
^{42}Ca	0.647	$^{40}Ar^{1}H_2^{+}$	2200
		$^{14}N_3^{+}$	830
^{43}Ca	0.135	$^{14}N_3{}^{1}H^{+}$	740
^{44}Ca	2.086	$^{12}C^{16}O_2^{+}$	1280
		$^{14}N_2{}^{16}O^{+}$	965
		$^{88}Sr^{++}$	16500
^{46}Ca	0.004	$^{46}Ti^{+}$	43400
^{48}Ca	0.187	$^{48}Ti^{+}$	10500

High mass resolution enables $\delta^{44}Ca/^{43}Ca$, $\delta^{44}Ca/^{42}Ca$, and $\delta^{48}Ca/^{42}Ca$ values to be measured with external reproducibilities better than ±0.2‰ (2 s) from purified 10 ppm solutions of Ca-containing materials [22]. Except for $^{88}Sr^{++}$, $^{46}Ti^{+}$, and $^{48}Ti^{+}$, all interferences can be resolved using the medium resolution mode of the Finnigan NEPTUNE.

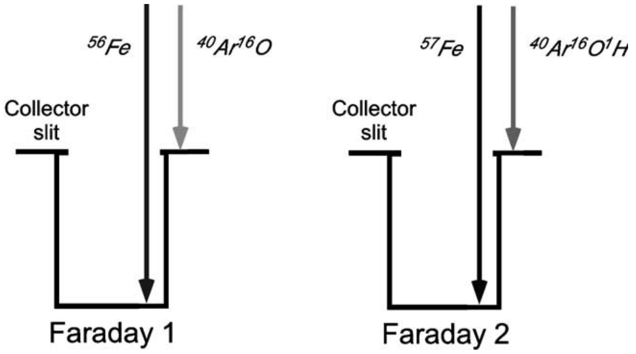

Fig. 17. Schematic presentation of the collector setup used for the simultaneous measurement of ^{56}Fe and ^{57}Fe using a high-resolution entrance and low-resolution collector slits. The resolved Fe isotopes are simultaneously collected at the edge position of the Faraday cups, while the polyatomic interferences do not enter the detectors (modified from [23]).

The practical mass resolution of this configuration is defined as the *resolving power* and given in Eq. (6) [23] where m(5%) is the mass at 5% of the peak height and m(95%) is the mass at 95% of peak height and m is the mass of the peak (Fig. 18):

$$R_{\text{power}}(5\%,\ 95\%) = \frac{m}{m(5\%) - m(95\%)} \tag{6}$$

The Finnigan NEPTUNE is capable to reach a resolving power of about R_{power} (5 and 95%) = 10,000 at a relative transmission of >5%. This is sufficient to safely separate molecular interferences with flat top peak sections, which would require a mass resolution of about 3500 for complete peak separation with triangular peak shapes.

The Isoprobe (introduced by Micromass and now marketed by GV Instruments) employs a hexapole collision cell to reduce the energy spread of the ions and to decompose some molecular interferences through ion–molecule collisions. A gas (such as Ar, He or H_2) is bled into the collision cell. The hexapole is operated with an RF field to focus the analyte ions to collide with the gas. In this manner, the ions lose kinetic energy and are “thermalized”. Some polyatomic ions, for example Ar-hydrides and oxides such as $^{40}Ar^{1}H_2{}^{+}$ or $^{40}Ar^{16}O^{+}$ create significant isobaric interference for $^{42}Ca^{+}$ and $^{56}Fe^{+}$, respectively. These molecular interferences are converted in the collision cell to species that do not interfere with the measurement. In general, the collision cell attenuates but not completely eliminates the interferences and there is still the need for high mass resolution. In some cases even new molecular compounds maybe formed in the collision cell. The latest version of the Isoprobe has high mass resolution capabilities as well.

Other methods to specifically reduce Ar-based polyatomic interferences include the use of low-power (or “cold”) plasma, for example at 300 W instead of 1200 W. Because the first ionization potential of Ar is high relative to many other elements, the proportion of Ar is greatly reduced while the sensitivity of the element of interest is affected to a lesser extent. The reduction in plasma power, however, makes the ion source more sensitive to changes in the composition of the aerosol. The sensitivity and mass bias of the measurement become increasingly dependent on the concentration of the element, type and strength of the acid, and concentration of other ions in the solution analyzed. Thus, the cold plasma technique is of limited use for high precision isotope ratio measurements be-

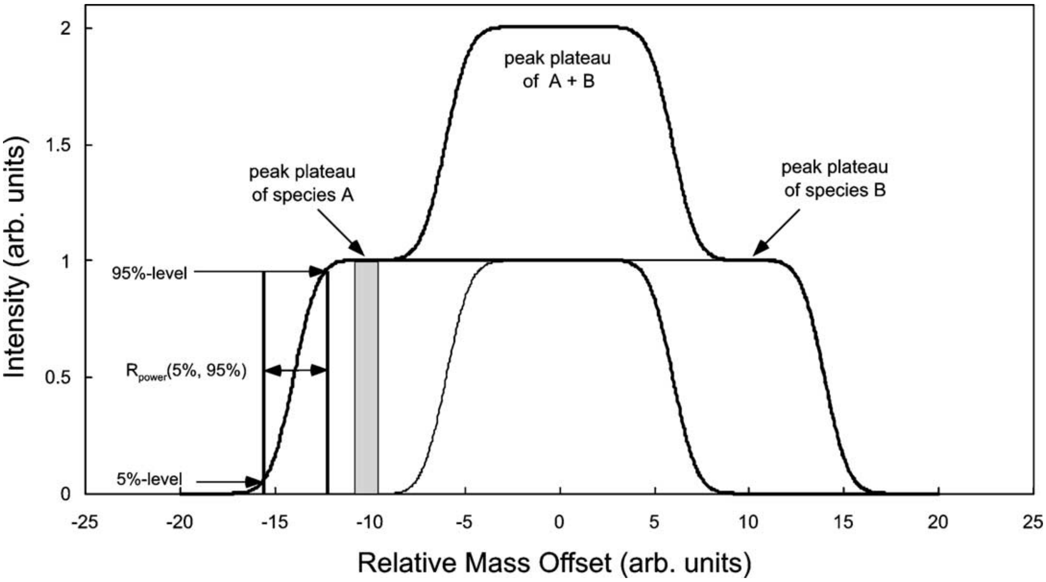

Fig. 18. Recorded peak profile when the adjacent ion beam profiles of ion species A and B with a mass difference of Δm are scanned across the low-resolution detector slit. First the lighter ion species A enters the detector slit and forms the first plateau section of the peak, which is indicated by the shaded rectangle. At that time, the heavier ion species B is still clipped at the high mass side of the detector slit. The second plateau section appears when both ion beams enter the detector slit. Finally, the ion beam A is clipped on the low mass side of the detector slit and only species B enters the cup and forms the third plateau section. The resolving power R_{power} (5 and 95%) is given by the distance of the two vertical lines (modified from [23]).

cause extreme care must be taken with respect to matrix effects.

4.2. *Internal normalization*

Instrumental mass bias alters the measured isotope abundances in both thermal ionization and inductively coupled plasma ion sources. Therefore, the result is not accurate and some correction to the data is typically applied to enable measurements made within one laboratory to be compared among different groups and also between TI-MS and MC-ICP-MS. The evaporation of the analyte from the heated metal filament in the TI-MS source leads to a depletion of the lighter isotope in the remaining sample. Thus, the ratio of the evaporated species changes in time, gradually becoming enriched in the heavier isotopes of the element as the measurement progresses. In the case of ICP-MS, the mass bias is primarily the result of space charge effects at the skimmer cone in the plasma torch. The absolute magnitude of mass bias effects is about ten times larger for ICP-MS (1% per mass unit in the high mass range) compared to TI-MS (on the order of 0.1% per mass unit in the high mass range).

The fractionation or mass bias effects can be corrected using one of many empirical mass fractionation laws. Many of these laws are based on empirical observations. Typically, the same TI-MS correction laws have been used for ICP-MS as well. However, since the instrumental fractionation mechanisms are completely different in the two ion sources, caution is required (Fig. 19). Compared to TI-MS, the mass-bias originating in the ICP source is less understood and there is still discussion as to its causes and how to best correct for its effects [24–26].

ICP-MS is a multiple element technique and it is possible to add an elemental spike to the sample and use this spiked element to correct for mass bias effects. An important example of this is the analysis of Pb where all isotopes, except ^{204}Pb, are radiogenic and no isotope pair can be used for internal normalization. One can employ a Tl spike (^{203}Tl and ^{205}Tl) during the measurement of Pb isotopes (^{204}Pb, ^{206}Pb, ^{207}Pb, and ^{208}Pb). The isotope abundance ratio of the elemental spike is known and the extent of fractionation can be calculated according to an empirical power or exponential law. The resulting fractionation factor for Tl is then applied to the isotopes of Pb. The advantage of this internal standardization is that the mass bias is monitored continuously and can be used to correct for differences in the matrix among different samples, as the matrix will affect the mass bias. However, the mass bias of the ICP source depends not only on the mass of the ion, but also on the chemical nature of the ion and the matrix. Thus, inaccuracies may result because the spike and analyte elements have slightly different chemical characteristics and because of matrix effects.

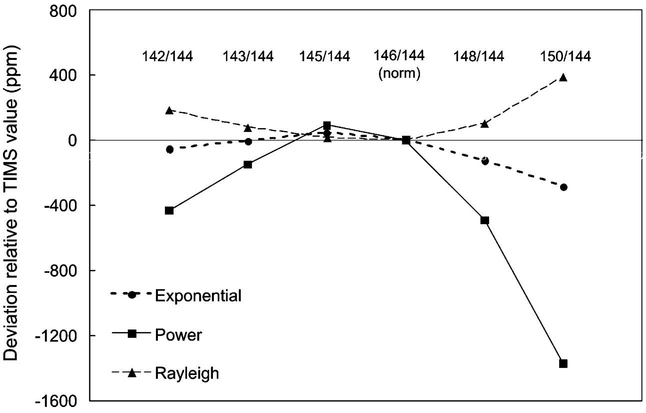

Fig. 19. The relative deviation of an isotopic Nd standard measured with the Finnigan NEPTUNE and evaluated with three different accepted fractionation "laws". The TI-MS values of the isotopic Nd standard are taken as a reference. The "power law"results in a systematic under correction over the mass range while the "exponential law" and the "Rayleigh law" seems to give a closer agreement between absolute TI-MS data and ICP-MS data.

4.3. *External normalization using standards*

Another approach to correct for mass bias is "standard-sample bracketing" where the measurement of the unknown is preceded and followed by the measurement of a standard. Correction of mass bias by standard-sample bracketing requires that there is a monotonic increase or decrease in the mass bias during the analytical sequence. The isotope abundance ratios of the sample are compared to the measured values of the isotope abundance ratios of the standard using a delta (δ) or epsilon (ε) value scale according to Eq. (7). Delta values express the deviations in the isotope composition of the sample relative to the standard in parts per thousand (or permil) whereas epsilon values are expressed as parts per ten thousand. No assumptions must be made regarding the functional form of the mass bias effects and they cancel out in the calculation. For example, ^{57}Fe/^{54}Fe isotope abundance ratios can be expressed as δ^{57}Fe values relative to the Fe standard reference material IRMM-014 distributed by the Isotope Reference Materials Measurement laboratory in Geel, Belgium (Eq. (7)):

$$\delta^{57}\mathrm{Fe}(‰) = \left(\frac{(^{57}\mathrm{Fe}/^{54}\mathrm{Fe})_{\mathrm{sample}}}{(^{57}\mathrm{Fe}/^{54}\mathrm{Fe})_{\mathrm{IRMM-014}}} - 1 \right) \times 1000 \qquad (7)$$

Results expressed as delta or epsilon values are dependent on the choice of reference material.

For many elements, the rapid development and application of MC-ICP-MS resulted in the use of standard materials that were not widely distributed and were of unknown isotope composition. Published data were reported relative to solutions of high purity metals or elements derived from presumably homogenous reservoirs. This raises some potential problems. For example, high purity metals prepared by high temperature processes can result in an abnormally fractionated end product. Thus, this type of standard may not be representative of the element's terrestrial isotope composition. Also, elemental separation from natural materials may involve a process, such as ion exchange chemistry, that will fractionate the element's isotopes if less than 100% recoveries are realized. Recently, a group of researchers in collaboration with the IAEA prepared and circulated an extensive series of boron isotope reference materials for inter-laboratory measurement and comparison. Generally, it was observed that agreement was very good for measurements made by positive ion TI-MS (using $Cs_2BO_2^+$ ions) and acceptable for data obtained by negative ion TI-MS. However, some ICP-MS data were not included in the report because the deviations from the TI-MS data were large [27,28]. Beside the availability of calibrated standards it should be emphasized as a general statement that matrix effects should be considered carefully.

5. Emerging applications involving multiple collection

The MC-ICP-MS has great potential for measuring isotope abundances from transient signals generated by any number of peripheral devices. The mass spectrometer functions as an on-line isotope ratio monitor. The conversion of samples to a form suitable for direct measurement is realized using elemental analyzers, chemical reactors, HPLC, GC, and lasers.

5.1. Laser ablation (LA-MC-ICP-MS)

Most conventional isotope analyses involve the dissolution of relatively large quantities of sample followed by some form of purification to isolate the element of interest. Often this requires that the sample is homogenized and detailed information over micrometer distances is lost. High-resolution sampling is desirable in many cases, for example, to date single zircons using U–Pb geochronometers, to correlate Sr deposited in human teeth related to the Sr contained in local food and water sources, and to determine the sources of sulfur in hydrothermal fluids that formed sulfide minerals. The laser ablation (LA) probe eliminates the need to physically remove the region of interest from the sample matrix. Thus, sensitivity is increased while analytical blanks are reduced.

For example, the isotopes of U and Pb can be measured in individual zircon grains to determine the amount ^{207}Pb and ^{206}Pb that have accumulated in the zirconium silicate matrix from the natural radioactive decays of ^{235}U and ^{238}U, respectively. In one study, Bouman et al. [29] employed a 213 nm wavelength laser focused to a 20 μm spot on the surface of single zircons (Fig. 20). The laser was pulsed at 10 Hz with an average energy density of 25 J/cm^2. Helium carrier gas swept the aerosol from the sample chamber through a gold trap to remove trace amounts of Hg vapour in the He stream. The process gas was mixed with Ar prior to admission to the ICP source of the Finnigan NEPTUNE MC-ICP-MS. Multiple ion-counters were employed to measure the small amount of Pb produced from the ablated volume Four ion counters were positioned to collect ^{202}Hg, ^{204}Pb, ^{206}Pb, and ^{207}Pb. Simultaneous detection of ^{202}Hg and ^{204}Pb ensured that the Hg blank during the actual sample measurement was accurately accounted for and reliable common lead corrections could be made. Typical blank levels were 2000 cps for ^{202}Hg, 20–30 cps of ^{204}Pb, 250 cps ^{206}Pb, and 350 cps ^{207}Pb. A collector was also arranged for ^{238}U to check for concordant ages. Data were collected over a 70 s window. Six different locations on a 91500 zircon standard were analyzed and the average ^{207}Pb/^{206}Pb ratio had a standard deviation of ±0.22%. Three different zircons were measured and the results are summarized in Table 3. The LA-MC-ICP-MS data compare favorably with the recommended ages determined

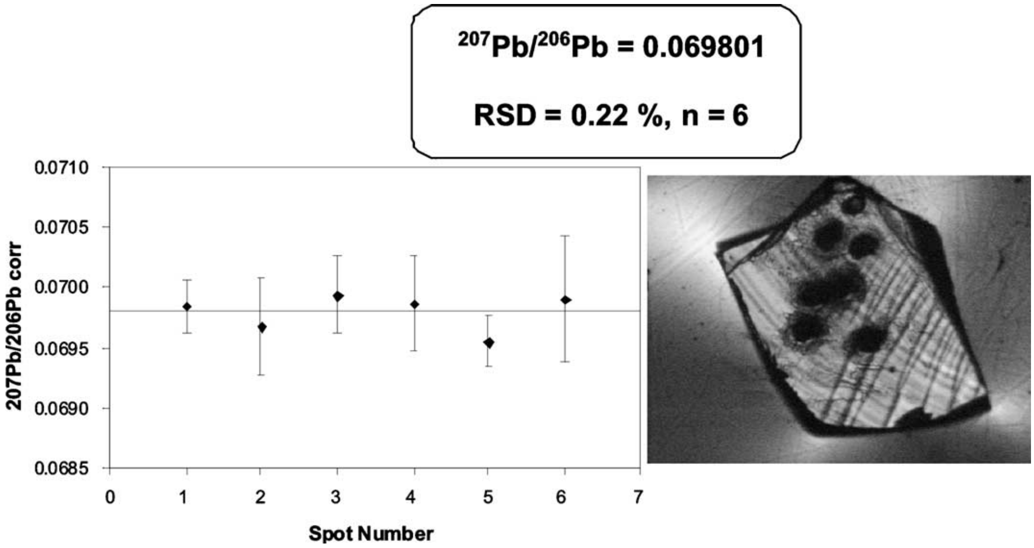

Fig. 20. The results of laser ablation multiple ion counting inductively coupled plasma mass spectrometric analysis of single zircon grains. The minute quantities of Pb and U released were swept into the source of a Finnigan NEPTUNE MC-ICP-MS equipped with multiple ion counters arranged to collect ^{202}Hg, ^{204}Pb, ^{206}Pb, ^{207}Pb, and ^{238}U (see Fig. 15; [29]).

Table 3
U–Pb ages determined by laser ablation multiple ion counting inductively coupled plasma mass spectrometry (LA-MIC-ICP-MS) for three zircon samples

Sample	LA-MC-ICP-MS determined age[a] (Ma)	Recommended age (Ma)
PMA-7	2390 ± 55 ($n = 3$ spots)	2430 ± 4
CN-92	1143 ± 12 ($n = 3$ spots)	1143.0 ± 0.5
5-FRATI	290 ± 7 ($n = 6$ spots)	286 ± 3

The recommended ages were determined using conventional TI-MS techniques [29].

[a] All uncertainties are reported at the 2σ level.

on separated Pb and U measurements using TI-MS even for relatively young zircons (i.e., zircons with very low amounts of radiogenic Pb).

5.2. *Hydride generation (HG-MC-ICP-MS)*

Hydride generation improves the sensitivity for elements that are difficult to ionize in the ICP source [30]. The element to be analyzed is dissolved in an acidic solution and mixed with a reducing agent (i.e., $NaBH_4$) to form a covalent hydride (i.e., H_2Se, H_2Te or GeH_4). The volatile analyte is separated from the byproducts of the reaction in a gas-liquid separator in the presence of a stream of Ar carrier gas. The sample gas is then input to the ICP source (Fig. 21). For example, the concentration of Se in many biologic and geologic reservoirs is typically below 1 ppm [31]. Rouxel et al. [32] analyzed as little as 10 ng of Se with external precisions in the $^{82}Se/^{76}Se$ isotope abundance ratio of 0.25 ‰ (2σ). This compares very favorably with negative ion TI-MS methods where $^{80}Se/^{76}Se$ ratios were measured with precisions of ± 0.2 ‰ at 2σ confidence limits from 500 ng of Se [33]. Recently, Rouxel et al. [34] have reported on the analysis of Sb by hydride generation (SbH_3) coupled to MC-ICP-MS. They achieved an external precision of ±0.4 ε (95% confidence level) from tens of nanograms of Sb. Thus, they were able to identify Sb isotope fractionations during the reduction of Sb(V) to Sb(III) as well as isotope abundance variations among continental/oceanic crusts and hydrothermal environments that they suggest reflect contributions from Sb sources and possibly kinetic fractionations as Sb is reduced in low temperature environments.

5.3. *Separation of liquid or gaseous mixtures by HPLC or GC*

The combination of a liquid or gas chromatograph with the multicollector ICP-MS has great potential to reveal reaction mechanisms as an element undergoes complex chemical conversions. Whereas bulk decomposition converts all chemical forms of the element of interest to a single compound, chromatographic methods preserve the isotope composition of individual compounds in complex mixtures. This is particularly important because trace organometallic compounds have characteristic mobilities, bioavailabilities, and toxicities that distinguish them from inorganic compounds [35]. Passing the sample through some form of chromatographic column ensures that the analyte is separated from the matrix, all interfering elements are separated from one another and the sample is preconcentrated in the column. For example, Krupp et al. [36] demonstrated the feasibility of this technique by analyzing $PbEt_4$ that was synthetically derivatized from a solution of the NIST 981 Pb isotope standard (Fig. 22). The sample was injected into an HP 6850 capillary GC interfaced to a Thermo Elemental Axiom MC-ICP-MS. A Tl spike was introduced simultaneously to correct for mass bias. The ^{206}Pb, ^{207}Pb, ^{208}Pb isotope abundance ratios were measured with precisions of 0.07% RSD. The $^{208}Pb/^{206}Pb$, and $^{208}Pb/^{204}Pb$ ratios were measured with accuracies of 0.18 and 0.9%, respectively. Krupp et al. [37] recently applied the capillary gas chromatography to the analysis of sulfur isotope abundances by MC-ICP-MS. Using SF_6, they achieved precisions for $^{32}S/^{33}S$ and $^{33}S/^{34}S$ better than 0.4% R.S.D. The ability to measure sulfur isotope abundances in separated inorganic and organic fractions is critical in order to distinguish between sulfur of biogenic compared to anthropogenic activities. Speciation analyses, particularly for elements of biological significance (i.e., S, Ca, and Fe), is the next frontier for isotope research and will extend this powerful technique to new areas including Medical Science where radioactive tracers are currently employed.

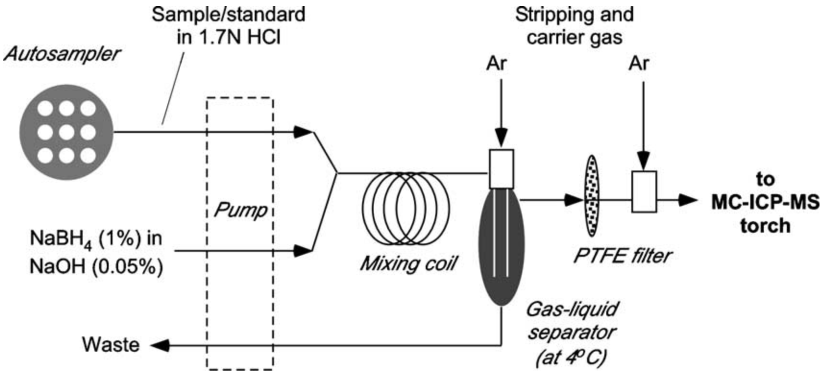

Fig. 21. Hydride generation can be used to improve the sensitivity for elements that are difficult to ionize in the ICP source. In this case, Se is mixed with a reducing agent to form a covalent hydride. The product of the reaction is dried and swept into the ICP source (modified from [31]).

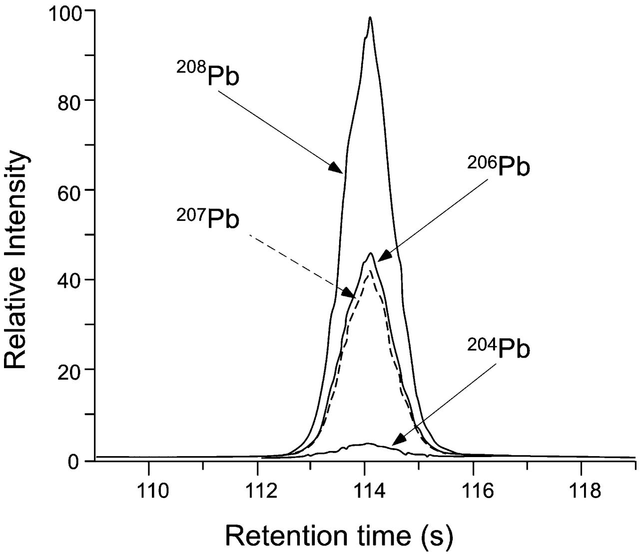

Fig. 22. Ion current intensities of lead isotopes from $PbEt_4$ plotted as a function of time measured by an Axiom MC-ICP-MS. The $PbEt_4$ was eluted from a chromatographic column. Relative Pb isotope abundances in this particular fraction can be calculated by taking ratios of the areas underneath each of the curves (modified from [36]).

Günther-Leopold et al. [38] combined an HPLC with an MC-ICP-MS to determine the extent of nuclear reactions based on the fission of ^{235}U and ^{239}Pu and the production of ^{148}Nd in nuclear fuels. Conventional high precision measurement requires that the different radioactive elements are chemically separated from the matrix and analyzed individually. This is not only a tedious procedure, but the technician also faces the risk of exposure to high doses of radioactivity. In contrast, separation by HPLC is simple and rapid. The sample introduction peripherals were housed in a glove box to isolate the operator from the radioactive compounds. Samples were injected to a Dionex HPLC equipped with a CG5A guard column and CS5A analytical column interface to a Finnigan NEPTUNE MC-ICP-MS. Internal normalization of nuclear fuel samples is not possible because the isotope abundance ratios are very different from natural values. Therefore, standard sample bracketing methods were employed and the standard was also injected on the HPLC column. In this manner, the matrix was identical for both sample and standard.

6. Conclusion

The magnetic sector mass spectrometer has evolved into a sophisticated high resolution, multicollector instrument capable of measuring isotope abundance variations with extreme levels of precision and, if carefully applied, accuracy. Thoughtful and imaginative engineering has produced instrumentation that is relatively simple to operate, yet can reveal information that cannot be gathered by any other analytical technique. Improvements in detector technology from analog current amplifiers to sophisticated ion counting detectors open the possibility to analyze smaller and smaller sizes. Elimination of cross calibration errors resulted in the resolution of minute isotope abundance variations as small as a few ppm.

It appears that both TI-MS and MC-ICP-MS will both continue to have a place in the isotopist's toolbox. These are both complimentary techniques. One of the most important distinctions is that the ICP source is an atmospheric ionization source in which the sample can be introduced directly under atmospheric pressure. This makes it an ideal tool to develop high precision on-line techniques in combination with laser ablation or novel hyphenated methods including GC and LC that enable new opportunities in isotope analysis measurements. A broader spectrum of scientists from different fields of applications will use multiple collector mass spectrometers to investigate isotope effects of an increasing number of elements. Careful and precise measurements are revealing isotope abundance variations for elements that play significant roles in biological, geological, nuclear and chemical processes. For example, stable isotope abundance data for elements such as Ca, Fe, Ni, Zn, and Mo may prove essential in understanding metabolic pathways and possibly be applied in clinical treatments.

References

[1] S.J.G. Galer, H.J. Laue, S.L. Goldstein, K. Metzger, A.W. Hofmann, A. Tegtmeyer, M. Wegner, EUG 8, Strasbourg, Abstract Supplement No. 1, Terra Nova, 7, 1995.
[2] N.S. Belshaw, P.A. Freedman, R.K. O'Nions, M. Frank, Y. Guo, Int. J. Mass Spectrom. 181 (1998) 51.
[3] T.M. Esat, Int. J. Mass Spectrom. 148 (1995) 159.
[4] S. Richter, S.A. Goldberg, P.B. Mason, A.J. Traina, J.B. Schwieters, Int. J. Mass Spectrom. Ion Proc. 206 (2001) 105.
[5] N.R. Daly, Rev. Sci. Instrum. 31 (1960) 264.
[6] M.G. Inghram, R.J. Hayden, A Handbook on Mass Spectroscopy, Nuclear Science Series Report No. 14, National Academy of Sciences-National Research Council, Washington, DC, 1954.
[7] N.S. Belshaw, R.K. O'Nions, F. von Blanckenburg, Int. J. Mass Spectrom. Ion Proc. 142 (1995) 55.
[8] N.J. Freeman, N.R. Daly, R.E. Powell, J. Sci. Instrum. 38 (1967) 945.
[9] P. Van Calstern, J.B. Schwieters, Int. J. Mass Spectrom. Ion Proc. 146/147 (1995) 119.
[10] K. Habfast, H.-J. Laue, US Patent 5,043,575, issued 14/02/1990.
[11] T. Lee, T.-L. Ku, H.-L. Lu, J.-C. Chen, Geochim. Cosmochim. Acta 57 (1993) 3493.
[12] K. Ludwig, Chem. Geol. 135 (1997) 325.
[13] B. Luais, P. Telouk, F. Albaréde, Geochim. Cosmochim. Acta 61 (1997) 4487.
[14] J. Schwieters, H. Lerche, Method for measuring ionic currents, and a catching device, Thermo Electron (Bremen), US Patent 6,472,659 B1, issued 29/10/2002.
[15] C.L. Harper, S.B. Jacobsen, Nature 360 (1992) 728.
[16] M. Sharma, D.A. Papanastassiou, G.J. Wasserburg, R.F. Dymek, Geochim. Cosmochim. Acta 60 (1996) 2037.
[17] G. Caro, B. Bourdon, J.-L. Birck, S. Moorbath, Nature 423 (2003) 428.
[18] G. Caro, B. Bourdon, J.-L. Birck, S. Moorbath, Geochim. Cosmochim. Acta 68 (Suppl. 1) (2004) A746.

[19] J.B. Schwieters, C. Bouman, D. Tuttas, M.E. Wieser, Geochim. Cosmochim. Acta 68 (Suppl. 1) (2004) A60.
[20] A.J. Walder, P.A. Freedman, J. Anal. Atom. Spectrom. 7 (1992) 571.
[21] T. Walczyk, Anal. Bio. Chem. 378 (2003) 229.
[22] M.E. Wieser, D. Buhl, C. Bouman, J. Schwieters, J. Anal. Atom. Spectrom. 19 (2004) 844.
[23] S. Weyer, J.B. Schwieters, Int. J. Mass Spectrom. 226 (2003) 355.
[24] F. Albarède, P. Telouk, J. Blichert-Toft, M. Boyet, A. Agranier, B. Nelson, Geochim. Cosmochim. Acta 68 (2004) 2725.
[25] C.P. Ingle, B.L. Sharp, M.S.A. Horstwood, R.R. Parrish, D.J. Lewis, J. Anal. Atom. Spectrom. 18 (2003) 219.
[26] M.F. Thirwall, R. Anczkiewicz, Int. J. Mass Spectrom. 235 (2004) 59.
[27] R. Gonfiantini, S. Tonarini, M. Gröning, A. Adorni-Braccesi, A.S. Al Ammar, M. Astner, S. Bächler, R.M. Barnes, R.L. Bassett, A. Cocherie, A. Deyhle, A. Dini, G. Ferrara, J. Gaillardet, J. Grimm, C. Guerrot, U. Krähenbühl, G. Layne, D. Lemarchand, A. Meixner, D.J. Northington, M. Pennisi, E. Reiznerová, I. Rodushkin, N. Sugiura, R. Surberg, S. Tonn, M. Wiedenbeck, S. Wunderli, Y. Xiao, T. Zack, Geostand. Newslett. 27 (2003) 41.
[28] S. Tonarini, M. Pennisi, A. Adorni-Braccesi, A. Dini, G. Ferrara, R. Gonfiantini, M. Wiedenbeck, M. Gröning, Geostand. Newslett. 27 (2003) 21.
[29] C. Bouman, A. Cocherie, M. Robert, J.B. Schwieters, M.E. Wieser, Geochim. Cosmochim. Acta 67 (Suppl. 1) (2003) A44.
[30] P. Pohl, Trends Anal. Chem. 23 (2004) 87.
[31] T. Johnson, Chem. Geol. 204 (2004) 201.
[32] O. Rouxel, J. Ludden, J. Carignan, L. Marin, Y. Fouquet, Geochim. Cosmochim. Acta 66 (2002) 3191.
[33] T. Johnson, M. Herbel, T.D. Bullen, P.T. Zawislanski, Geochim. Cosmochim. Acta 18 (1999) 2775.
[34] O. Rouxel, J. Ludden, Y. Fouquet, Chem. Geol. 200 (2003) 25.
[35] M. Moldovan, E.M. Krupp, A.E. Holliday, O.F.X. Donard, J. Anal. Atom. Spectrom. 19 (2004) 815.
[36] E.M. Krupp, C. Pécheyran, H. Pinaly, M. Motelica-Heino, D. Koller, S.M.M. Young, I.B. Brenner, O.F.X. Donard, Spectrochim. Acta B 56 (2001) 1233.
[37] E.M. Krupp, C. Pécheyran, S. Meffan-Main, O.F.X. Donard, Anal. Bioanal. Chem. 378 (2004) 250.
[38] I. Günther-Leopold, B. Wernli, Z. Kopajtic, D. Günther, Anal. Bioanal. Chem. 378 (2004) 241.